

This is a preprint of a paper intended for publication in a journal or proceedings. Since changes may be made before publication, this preprint is made available with the understanding that it will not be cited or reproduced without the permission of the author.

UCRL - 77151
PREPRINT
Conf. - 75/088-1



LAWRENCE LIVERMORE LABORATORY
University of California/Livermore, California

A Charged-Particle Magnetic-Quadrupole Spectrometer
for Neutron Induced Reactions*

R. C. Haight
S. M. Grimes
B. J. Tuckey
J. D. Anderson

December 10, 1975

MASTER

NOTICE
This report was prepared as an account of work sponsored by the United States Government under the United States and the United States Energy Research and Development Administration, not any of its contractors, employees, or any of their contractors, servants, agents or employees, makes any liability or responsibility for the accuracy, completeness or inclusion of any information, apparatus, product or process disclosed, or represents that its use would not infringe privately owned rights.

This paper was prepared for presentation at the APS Meeting
in Austin, Texas, October 30-November 1, 1975

DISTRIBUTION STATEMENT UNCLASSIFIED

A Charged-Particle Magnetic-Quadrupole Spectrometer
for Neutron Induced Reactions*

R. C. Haight, S. M. Grimes, B. J. Tuckey, and J. D. Anderson
Lawrence Livermore Laboratory, Livermore CA 94550

Abstract

A spectrometer has been developed for measuring the charged particle production cross sections and spectra in neutron-induced reactions. The spectrometer consists of a magnetic quadrupole doublet which focuses the charged particles onto a silicon surface barrier detector telescope which is 2 meters or more from the irradiated sample. Collimators, shielding, and the large source-to-detector distance reduce the background enough to use the spectrometer with a 14-MeV neutron source producing $4 \cdot 10^{12}$ n/s. The spectrometer has been used in investigations of proton, deuteron, and alpha particle production by 14-MeV neutrons incident on various materials. Protons with energies as low as 1.1 MeV have been measured. The good resolution of the detectors has also made possible an improved measurement of the neutron-neutron scattering length from the 0° proton spectrum from deuteron breakup by 14-MeV neutrons.

*Work performed under the auspices of the U. S. Energy Research and Development Administration under Contract W-7405-ENG-48.

I. Introduction

The problems of low signal-to-background ratios have traditionally interfered with the measurement of the cross sections and spectra of charged particles produced in 14-MeV neutron-induced neutrons. The low ratios result both from low true counting rates as well as from high background rates, and each is a function of several factors.

The signal is low for two reasons:

- (S1) Neutron source strengths are many orders of magnitude lower than charged particle beam intensities. A typical 14-MeV source strength is 10^{10} to 10^{11} n/s into 4π which can provide a flux of $\sim 10^8$ n/cm²-sec on the sample to be irradiated, the "radiator."
- (S2) Radiator thicknesses must be thin to allow the charged particles to escape with little energy loss. For example, a 2 MeV proton loses 200 keV in 1.7 mg/cm² of aluminum. This thickness is only $3.8 \cdot 10^{-5}$ atoms/barn. A cross section of 10 mb/sr and a solid angle of 10^{-3} sr therefore yield a probability of production of the charged particle of $3.8 \cdot 10^{-10}$ per incident neutron into this solid angle.

The background is more complicated but can be analyzed as two components:

- (B1) Charged particles produced by neutron induced reactions in materials near the radiator constitute one source of background. This component has been reduced in previous work by the use of materials which do not produce many charged particles, e.g. lead, and by suitable collimation.
- (B2) Neutrons and gamma rays can interact in the detector and lead to a much larger background. Of course, this background is dependent on the type of detector. An example for detectors containing

hydrogen compounds (i.e. photographic emulsions or proportional counters with CH_4) is elastic scattering $^1\text{H}(n,p)n$ in which an energetic proton is produced and can look like an energetic proton from the radiator. In silicon detectors $\text{Si}(n,p)$ and $\text{Si}(n,\alpha)$ reactions are a source of background. Gamma rays on the other hand usually interact with the electrons of the detector and can cause very high singles rates in a counter.

To increase the signal and reduce the background a spectrometer has been developed for use with the LLL intense neutron source, which produces $4 \cdot 10^{12}$ n/s and effectively solves the source problem (S1). The basic component is a magnetic quadrupole doublet lens that focuses charged particles from the radiator onto the detector. The solid angle for detection is thereby enhanced and compensates in part for the thin radiator (S2). The spectrometer is directional in the sense that the charged particles traverse well known paths through the quadrupole magnet. With suitable collimators the spectrometer does not "see" the materials near the radiator and hence background (B1) is essentially eliminated. Finally, the large neutron source-to-detector separation reduces the neutron and gamma-ray flux at the detector by the $1/r^2$ solid angle factor and allows more shielding to be placed between the source and the detector. The background (B2) is thereby substantially reduced.

Magnetic quadrupole lenses have been used by several groups to focus low energy (< 50 MeV) charged particle reaction products onto energy-detecting counters. O'Connell et al.⁽¹⁾ used a quadrupole triplet lens to measure the charged particles from photonuclear reactions. Although the charged particle optics of their quadrupole triplet are much different from a quadrupole doublet, their use of the spectrometer to enhance the signal and to reduce the background is similar to ours. Spectrometers

containing magnetic quadrupole doublet lenses have also been described⁽²⁻⁴⁾ for measuring charged particles from charged particle induced reactions. While these spectrometers have large solid angles, they have been used to a large extent to remove an unwanted but prolific charged particle species, a problem which is not present in neutron-induced reactions. The backgrounds in both the photonuclear and charged particle beam studies are quantitatively different from those encountered with an intense neutron source.

2. Apparatus

The spectrometer consists of a magnetic quadrupole doublet lens, a silicon surface barrier counter telescope, an evacuated transport pipe and suitable collimators and shielding. It is used in conjunction with a reaction chamber and with the Lawrence Livermore Laboratory's intense 14-MeV neutron source (ICT) which has produced intensities of $4 \cdot 10^{12}$ n/s. The layout of the spectrometer is given in Fig. 1.

The sequence of events is as follows. The 14-MeV neutrons are produced when a deuteron beam (D^+) impinges on a rotating tritiated titanium target.⁽⁵⁻⁷⁾ This source is nearly ($\pm 10\%$) isotropic and monoenergetic (to ± 1 MeV). It can be located at, for example, positions 1, 2, 3, 4, or 5 on Fig. 1. Some of the source neutrons impinge on the material to be investigated. This material is called the radiator and it is mounted in a reaction chamber. Charged particles which are produced by interactions between the neutrons and the radiator and which enter the transport tube are focused by the magnetic lens onto the detector telescope.

This arrangement increases the signal and decreases the background.

Because of the focusing properties of the magnetic lens, the effective solid angle for detecting charged particles is on the order of the solid angle subtended by the entrance aperture of the magnet. The detector subtends a much smaller solid angle for the background due to source neutrons and gamma rays which are produced in profusion by neutron interactions near the source. In addition, because of the large separation between the source and the detector, there is space for additional shielding to reduce these backgrounds even further. Another type of background is the charged particles which are produced elsewhere than in the radiator, for example, in the walls of the transport tube. Suitable collimation eliminates these unwanted charged particles.

The components of the spectrometer will now be discussed in detail.

2.1 Magnetic Quadrupole Doublet

The magnetic quadrupole doublet is an air-cooled, commercially supplied unit⁽⁸⁾ which had been purchased for another application in our Laboratory. It has an aperture of 12.4 cm. The lengths of the pole tips are 25.4 cm each and the pole tips of the two elements are separated by 17.7 cm. The effective field lengths as quoted by the manufacturer are 31.1 cm each and their separation is 12.1 cm. The maximum magnetic field at the pole tips is 2.3 kg and the maximum field gradient is 380 g/cm.

2.2 Detector Telescope

The detector telescope is a ΔE -E silicon surface barrier two detector telescope which is somewhat different in detail from those used in investigating charged-particle-induced reactions. It is mounted on one end of a stainless steel rod which extends through a ball joint outside the vacuum. The position of the detector can therefore be adjusted by moving this rod until the detector is at the focus of the magnetic lens.

An alpha-particle source placed at the radiator position serves as the source of charged particles to be focused and detected in this set-up procedure.

Three telescopes have been used to date. For measurements of protons above 6 MeV and deuterons above 8 MeV, the telescope consisted of a 150 μm by 300 mm^2 ΔE detector and a 1500 μm by 200 mm^2 E detector. The larger ΔE detector insured that its edges would not stop any particles traveling toward the E detector. Tantalum collimators of 18 mm diameter for the ΔE detector and 15 mm diameter for the E detector were used to avoid edge effects in the charge collection. The collimator for the ΔE detector was placed behind the detector because the detector mount consisted in part of epoxy and teflon. The former definitely contains hydrogen and the latter could contain hydrogen that would contribute to the background via the large $^1\text{H}(n,p)n$ elastic scattering cross section. (Despite the shielding, some neutrons do reach the detectors.) The recoil protons would be detected with a very large solid angle. Protons from the $^{19}\text{F}(n,p)^{19}\text{O}$ reaction in teflon could be another source of background. The collimator dimensions and locations were designed to prevent the protons produced in such events from being detected in both detectors.

The other telescopes we have used consist of a 1500 μm by 50 mm^2 E detector and either a 50 μm by 50 mm^2 or a 15 μm by 50 mm^2 ΔE detector. The latter has allowed the measurement of protons with energies as low as 1.1 MeV, deuterons as low as 1.4 MeV, and alpha particles down to 3.5 MeV. The tantalum collimators for these telescopes have apertures of 7 mm and are oriented as for the large telescope.

Another feature of these telescopes which differentiates them from conventional telescopes is that the ΔE and E detectors must be separated to reduce another source of background. The neutrons which reach the

detectors can induce an (n,p) , $(n,n'p)$, or (n,α) reaction in the silicon of one detector. The charged particle may then be detected by the other detector. This event will satisfy the coincidence requirement. If the event takes place at the proper location in one of the detectors, the event will also have the particle identification signature of one of the particles of interest. Because of the large cross sections for these reactions on all of the silicon isotopes, these events can produce a large counting rate. If the separation between the detectors is increased, however, the solid angle for one detector relative to the other is reduced significantly and hence the number of such events satisfying the coincidence requirement is likewise reduced. For the 50 mm^2 detectors a separation of 3 cm is usually adequate whereas the larger detectors must be separated by 8 cm or more. This type of background is another justification for the location of the tantalum collimators relative to their respective detectors.

2.3 Collimators

Collimation near the radiator and inside the transport tube is important in reducing background. Immediately downstream from the 2.5 cm diameter radiator, a lead collimator (C1 in Fig. 1) with a 2.2 cm circular aperture prevents charged particles born in the radiator frame, the radiator mounting wheel and much of the reaction chamber from traveling into the transport tube. At the entrance to the magnet, a lead collimator (C2 in Fig. 1) with an oblong aperture intercepts some of the charged particles produced in the reaction chamber walls and in the walls of the transport tube. None of the charged particles from the radiator which would pass through the magnet are intercepted by this collimator. The lead collimator (C3) at the exit of the magnet is identical to C2 but rotated 90° to pass the charged particle envelope from the radiator.

The transport tube itself also acts as a collimator. It is 10 cm in diameter and is lined with lead to reduce background.

The lead collimators and the lead liners are cleaned prior to use to remove contaminants. In particular, hydrocarbons must be removed to eliminate recoil protons from $^1\text{H}(n,p)n$ elastic scattering. The cleaning procedure we use is to immerse the components in nitric acid (diluted 10:1 with distilled water) for almost one minute, rinse with distilled water, and then polish the surface with a tissue.

In the middle of the quadrupole doublet there is a 2.54 cm diameter by 43 cm long copper shadow bar that serves four purposes. First, it intercepts particles traveling in the zero magnetic field region and thereby sharpens the momentum-selective characteristics of the magnet. Second, the shadow bar eliminates particles with unusual trajectories. Many of these particles are produced in the walls of the reaction chamber or transport tube and hence are an unwanted background. Third, the shadow bar acts as a necessary shield between the detectors and the neutron source when the source is placed at position 5 for zero-degree measurements. For 14-MeV neutrons, the bar is 10.9 mean free paths long and thus it provides good shielding for the detectors from the neutron source in this geometry. Fourth, the shadow bar shields the detectors from the gamma rays that are produced by neutron interactions near the source regardless of whether the source is at position 1, 2, 3, 4, or 5. These advantages of the shadow bar more than compensate for the 20% reduction in the transmitted particles.

2.4 Shielding

The detector must be shielded as much as possible from the source neutrons, from scattered neutrons and from gamma rays produced by neutron

interactions. These radiations can give unacceptably high counting rates in the detectors, and consequently, undesired accidental coincidences and dead time in the electronics. Furthermore, a fast neutron fluence of 10^{12} n/cm² significantly degrades the performance of silicon surface barrier detectors. An unshielded detector would receive this fluence in a few days at our source strengths.

The rather large separation between the neutron source and the detectors in this spectrometer offers much more flexibility for shielding than if the detector were closer to the radiator. We have not investigated all the possible shielding combinations but we have found some configurations that are especially effective.

The advantages of the copper shadow bar have been discussed in the preceding section. When the neutron source is at position 5 of Fig. 1, this shadow bar provides the only shielding of the detector from the source neutrons. When the neutron source is at position 1, 2, or 3, a rectangular prism 20.3 cm x 5.1 cm x 2.5 cm of tungsten alloy is placed inside the transport tube and to the left of collimator C2 in Fig. 1. Its longest dimension is parallel to the central ray and it is placed as near the transport tube wall as possible to intercept the neutrons from the source that travel toward the detector. This shield does not intercept charged particles from the radiator that otherwise would be detected.

A 5 cm thick by 10 cm long annular lead shield around the transport tube at the position of the detectors significantly reduces the gamma-ray and neutron background and consequently reduces the singles rates in the detectors.

Finally, we note that the quadrupole doublet itself acts as a good shield for certain orientations of the spectrometer relative to the source, for example, when the source is at position 4.

2.5 Reaction Chamber

The vacuum vessel of the reaction chamber consists of a 1.5 mm wall stainless steel cylinder, a 0.3 mm thick stainless steel end cap on one end and a more robust 6.3 mm thick plate on the other end. All sections of the chamber that can be seen by the spectrometer are lead lined to suppress the production of charged particles. The lead is cleaned prior to use as described previously. A small electric motor, a gear drive, and a mechanical rotating feed-through to rotate the radiator wheel are mounted on the plate. Up to ten radiator materials can be placed on the wheel and rotated successively into a position by remote control.

Care was taken to minimize the mass of the reaction vessel for two reasons. First, any excess mass in the vicinity of the neutron source can perturb the neutron flux spectrum at the radiator. The mass of the present reaction chamber is now less than the mass of the rotating target neutron source, however, and any further reduction is believed to be of little value. Second, the smaller the mass near the source, the smaller the radiological hazard in handling the apparatus at the end of the running period. Even with the small mass of our reaction vessel, the hazards associated with the activated material must be respected. For example, in three days of irradiation with the intense source at position 3, 1.2 cm from the wall of the reaction vessel, with an average source strength of $2 \cdot 10^{12}$ n/s, a hot spot several cm in diameter was produced on the wall. The long lived (primarily ^{60}Co) activity gave a $\beta + \gamma$

radiation level of 150 mR/hr at contact at this spot.

2.6 Supporting Structure

The entire spectrometer including the magnet, transport tube detectors reaction chamber, collimators and shielding are mounted on supports that are attached to a single aluminum plate. This plate is in turn supported by a specially designed assembly that allows movement in either of the two horizontal directions and also a rotation of the spectrometer about a vertical axis passing through the magnet. The vertical adjustment is accomplished by screw adjustments on the legs that support the entire spectrometer.

This flexibility of movement has proved very useful. In setting up for each running period, the spectrometer must be moved into position with little delay. The neutron source is fixed and the spectrometer must be aligned accurately. In the course of the measurements when the charged particle production angle is to be changed, the spectrometer is moved relative to the neutron source. For example, positions 1, 2, and 3 in Fig. 1 give production angles of 90°, 135°, and 45°, respectively. These angular changes are made by simply translating the entire spectrometer a few centimeters along its axis.

2.7 Vacuum System

A mechanical pump that produces a vacuum of 1.3 Pa (= 10 μ m Hg) has been adequate for this spectrometer. To minimize backstreaming of heavy hydrocarbons, a cold trap is placed between the pump and the evacuated volume of the spectrometer. Heavy hydrocarbons are to be avoided because they can lead to background through n-p elastic scattering.

3. Acceptance of the Spectrometer

The acceptance, a , of the spectrometer depends on the mass, m , charge, q , and energy, E , of the particle of interest. The acceptance can be written as the products of two quantities,

$$a(E,m,q) = \Omega(E,m,q) \epsilon(E,m,q)$$

where Ω is the probability measured in steradians that the magnet will focus the particle from the radiator onto the telescope and ϵ is the efficiency of the telescope. Ideally $\epsilon(E,m,q) = 1$ and $\Omega(E,m,q)$ can be calculated.

In practice ϵ can be less than unity especially for particles that deposit little energy in the ΔE or E detectors of the telescope. For example, in a 15 μm ΔE detector, ϵ is considerably less than unity for protons above 5 MeV which give a ΔE signal that approaches the electronic noise.

A more difficult problem is the calculation of $\Omega(E,m,q)$. A very good mapping of the magnetic field and excellent alignment of the system are required. Also, the distribution of reactions in the radiator must be known. In experiments where the source is at position 1, 2, or 3 there could be a significantly non-uniform production of charged particles because of the non-uniformity of the neutron flux.

We prefer therefore to measure $a(E,m,q)$ directly. The method is quick, simple and accurate. The spectrum of recoil protons is observed from elastic n-p scattering in a thick (3.2 mm) polyethylene radiator which has the same areal dimensions as the other radiators. The spectrum of protons $N(E)$ is proportional to

$$N(E_p) \sim \sigma(\theta, E_n, \text{proton}) \cdot \left[\frac{dE}{dx} (E_p) \right]^{-1} \text{CH}_2$$

for proton energies less than the end point, $E_{pmax} = E_n \cos^2 \theta$. Here $\sigma(\theta, E_n, p)$ is the n-p elastic scattering cross section in the laboratory for neutrons of energy E_n and for protons recoiling at a angle θ with respect to the incident neutron. The stopping power of polyethylene for protons of energy E_p is $\frac{dE}{dx}(E_p)$. The comparison of the observed spectrum with the expected spectrum yields $a(E, m, q)$

$$N_{obs}(E_p) = a(E, \text{proton}) N(E_p)$$

Similar measurements for deuterons from a thick deuterated polyethylene radiator and alpha particles from helium gas give $a(E, \text{deuteron})$ and $a(E, \alpha \text{particle})$. In cases where $a(E, m, q) = 1$, the acceptance can be deduced from the proton measurement alone since

$$\Omega_1(E_1, m_1, q_1) = \Omega_2(E_2, m_2, q_2)$$

$$\text{if } \frac{m_1 E_1}{q_1} = \frac{m_2 E_2}{q_2} \quad (\text{non-relativistically}).$$

A typical acceptance of the spectrometer is given in Fig. 2. The full width at half maximum (FWHM) of the energy band pass is $\frac{\Delta E}{E} = 39\%$ for this case where the large area detectors were used at a total radiator-to-detector distance of 3.74 m. For the smaller detectors, the band pass is smaller, typically $\frac{\Delta E}{E} = 20\%$ with a radiator-to-detector separation of 2.0 m.

4. Applications

The low background and high resolution characteristics of the spectrometer can be used separately or together. We give here three applications, the first of which uses primarily the low background feature whereas the second and third use both features.

4.1 Low Energy Protons from 14-MeV Neutron Bombardment of Materials

The entire proton production cross sections and spectra for 14-MeV neutrons incident on various materials are of interest for both basic and applied purposes. Recently the possibility of enhanced radiation damage by the hydrogen produced by (n,p) and $(n,n'p)$ reactions has been considered for the controlled thermonuclear reactors (CTR) of the future. The cross sections for hydrogen production by 14-MeV neutrons are not well known for many of the materials considered for CTR. In particular, the low energy part of the spectrum, which may contain many protons, is the most difficult to measure and is the most uncertain.

We have investigated the low energy proton production from several materials including aluminum. The radiator in this case was a thin 2.4 mg/cm^2 aluminum foil, the thickness chosen so that low energy protons would not stop in the foil itself. The telescope consisted of the $15 \text{ } \mu\text{m}$ ΔE detector and the $1500 \text{ } \mu\text{m}$ E detector. The raw spectra of radiator in and radiator out at the lowest magnet setting is given in Fig. 3. The peak of the acceptance function is at 1.5 MeV for protons. The foreground-to-background ratio integrated over the full width at one-third maximum is 14:1. The time to accumulate these data was slightly more than one hour.

The combined results of proton spectra measured at four magnet settings are given in Fig. 4. The full-width at half-maximum of the acceptance of the spectrometer for each of the magnet settings is given by the horizontal bars. The spectrum extends down to 1.1 MeV, which, to

our knowledge, is the lowest proton energy ever measured from 14-MeV neutrons incident on aluminum. The spectral shape above $E_p = 2.5$ MeV has the general features of previous measurements⁽⁹⁻¹³⁾ but is somewhat different in detail. The favorable signal-to-background ratio in this experiment should help to resolve previous discrepancies in the shape of this spectrum and its resolution into (n,p) and (n,n'p) contributions.^(9,10)

4.2 Proton Spectrum at 0° from Deuteron Breakup by 14-MeV Neutrons

The reaction $D(n,p)2n$ has been used to study the neutron-neutron final state interaction (fsi). From the proton spectrum measured at 0° , one can obtain, by a model-dependent analysis, the neutron-neutron scattering length, a quantity of fundamental importance in the study of the nucleon-nucleon interaction.

Many authors have studied this reaction at 14 MeV (see Ref. 14 and references therein) with results that differ by much more than the quoted errors. The success of this experiment depends on the statistical accuracy of the data and on the experimental resolution. Davis *et al.*⁽¹⁵⁾ have shown that, for an experimental resolution of 400 keV the statistical accuracy of the data must approach 3.3% for meaningful results. For a resolution of 200 keV, however, only 5.6% accuracy is required. The best resolution of a previous measurement appears to be 440 keV FWHM.⁽¹⁴⁾

This experiment was repeated with the present spectrometer. The experimental resolution of 200 keV FWHM was a factor of more than 2 better than even the best previous resolution. The source was located at position 5 of Fig. 1, 19 cm from the radiator and was operated to produce between 1.5 and $2.3 \cdot 10^{12}$ n/s. The angle between the 400 keV D^+ beam in the source and the central ray of the spectrometer was 98° which minimizes the neutron spread. At this angle the $\Delta E_n / \Delta E_{D^+}$ is a minimum which is important

because the deuterons can produce 14-MeV neutrons as they slow down from 400 keV to well below 100 keV in the TiT target. At this same angle, however, the $\Delta E_n/\Delta\theta$ ratio is nearly maximal. Consequently, the CD_2 radiator was in the shape of a strip 1.0 cm in width to limit $\Delta\theta$. The thickness of the radiator was 1.5 mg/cm^2 which was a compromise between good resolution and good counting rate. The radiator to detector distance was 3.74 m and the large area detectors were used in the telescope. A particle identifier gave a clean separation between protons and deuterons.

The proton spectrum from the CD_2 radiator clearly showing the neutron-neutron fsi peak at $E_p = 11.5 \text{ MeV}$ is given in Fig. 5. Again the horizontal bars denote the FWHM of the acceptance of the spectrometer for the three magnet settings. The value of the n-n scattering length derived from this spectrum is discussed at length elsewhere.⁽¹⁶⁾

4.3 Energy Resolution of the Source

For nuclear physics experiments, the energy distribution of the neutron source must be known and for some the width of the distribution must be minimized. The spectrometer was used to measure the neutron energy spread from the LLL intense neutron source for three incident D^+ energies to determine what energy resolution could be obtained. The spectrometer was set up as described in section 4.2 with a CH_2 radiator which was a thin strip, 5 mm wide to minimize the energy spread due to $\Delta E_n/\Delta\theta$. The thickness of the radiator was 0.6 mg/cm^2 . The contributions to the measured energy resolution were electronic (33 keV), $\Delta E_p/\Delta\theta_{np}$ ($< 20 \text{ keV}$) where θ_{np} is the proton recoil angle which was centered at 0° , energy loss in the radiator (20 to 25 keV) and $\Delta E_n/\Delta\theta$ in the neutron source. From geometrical considerations this last term was expected to be 24 keV

at $E_{D^+} = 200$ keV. The total energy spread of the detected protons obtained by adding these contributions in quadrature is about 50 keV. The measured resolution, however, was 114 keV (Fig. 6).

The explanation of this discrepancy is that small angle scattering of the D^+ beam as it slows down in the TiT target can increase $\Delta\theta$ significantly and hence can broaden the energy spread via the $\Delta E_n / \Delta\theta$ dependence. The resolution we observe at 200 keV D^+ is consistent with that measured by a completely different technique for another 14-MeV neutron source which, however, also consisted of a TiT target and a D^+ beam of only slightly lower energy, namely 175 keV.⁽¹⁷⁾ The previous results were explained by the Molière theory of multiple scattering.^(18,19)

At higher D^+ beam energies, the FWHM of the neutron energy spread at 98° is larger due to the expected increase in small angle multiple scattering. For $E_{D^+} = 300$ keV, a resolution of 163 ± 16 keV FWHM was measured. At $E_{D^+} = 400$ keV, however, the resolution improved slightly to 147 ± 16 keV FWHM. An explanation of these results depends significantly on the tritium distribution of the TiT target. Because the distribution changes in time and was not well characterized in these experiments, the significance of these experiments is not obvious. The general trend, however, invites further investigation.

Summary

A magnetic quadrupole lens which focuses charged particle reaction products onto detectors significantly improves the signal-to-background ratio for experiments on reactions induced by 14-MeV neutrons. The solid angle for detecting the desired charged particles is enhanced by the lens while that for detecting the background is reduced. The geometry also allows

sufficient shielding to reduce the singles counting rates to acceptable values and to minimize background events.

A spectrometer consisting of a magnetic quadrupole doublet lens, a silicon surface barrier detector telescope, collimators and shielding has been constructed for use with the LLL intense neutron source. Several successful measurements have been made with the spectrometer at $E_n = 14$ MeV. The $D(n,p)2n$ proton spectrum at 0° has been measured with a resolution of 200 keV. Low energy protons down to $E_p = 1.1$ MeV have been detected from the $Al(n, \alpha p)$ reaction. And an upper limit for the energy resolution of the neutron source has been determined through $^1H(n,p)n$ elastic scattering with a best overall resolution of the spectrometer of 114 keV.

REFERENCES

1. J. S. O'Connell, R. C. Morrison and J. R. Stewart, *Nucl. Instr. and Meth.* 30 (1964) 229.
2. R. E. L. Green and D. A. Lind, *Nucl. Instr. and Meth.* 94 (1971) 93.
3. G. W. Hoffmann, J. McIntyre, M. Mahlab and W. R. Coker, *Nucl. Instr. and Meth.* 120 (1974) 489.
4. G. R. Morgan, G. D. Gunn, M. B. Greenfield, N. R. Fletcher, J. D. Fox, D. McShan and L. Wright, *Nucl. Instr. and Meth.* 123 (1975) 439.
5. R. Booth, H. H. Barschall, and E. Goldberg, *IEEE Trans. Nucl. Sci.*, NS-20 (1973) 472.
6. R. Booth and H. H. Barschall, *Nucl. Instr. and Meth.* 99 (1972) 1.
7. R. Booth, *Nucl. Instr. and Meth.* 120 (1974) 353.
8. Alpha Scientific, Inc., 28971 Hopkins St., Hayward, CA 94544.*
9. K. R. Alvar, *Nucl. Phys.* A195 (1972) 289.
10. D. L. Allan, *Proc. Phys. Soc. (London)* A70 (1957) 195.
11. L. Colli, F. Cuelban, S. Micheletti, and M. Pignarelli, *Nuovo Cuento* 14 (1959) 81.
12. P. V. March and W. T. Morton, *Phil. Mag.* 3 (1958) 1256.
13. R. K. Haling, R. A. Peck, Jr., and H. P. Hubank *Pys. Rev.* 106 (1957) 971.
14. S. Shirato, K. Saitoh, N. Koori, and R. T. Cahill, *Nucl. Phys.*, A215 (1973) 277.
15. J. C. Davis, J. D. Anderson, S. M. Grimes and C. Wong, *Phys. Rev.* C8 (1973) 863.
16. R. C. Haight, S. M. Grimes, and J. D. Anderson (to be published).
17. M. Bormann and I. Richle, *Z. für Physik* 207 (1967) 64.
18. W. H. Breunlich, *Acta Physica Austriaca* 23 (1966) 224.
19. W. H. Breunlich, *Oesterr. Akad. Wiss., Math.-Naturwiss. Kl. Sitzungsber. Abt. II* 175 (1956) 1.

*Reference to a company or product name does not imply approval or recommendation of the product by the University of California or the U.S. E.R.D.A. to the exclusion of others that may be suitable.

FIGURE CAPTIONS

1. Schematic layout of the charged particle spectrometer. Possible neutron source positions are denoted by 1,2,...5. Cross sections of the collimators (C1, C2, C3) are detailed with an expanded scale ($\times 1.5$). Rotation of the radiator wheel is accomplished by a motor (M) and gears (G) and the position is read out by a potentiometer (P). F denotes Dependex flanges.
2. Acceptance of the quadrupole spectrometer with a 3.74 m radiator to detector separation and with the large area detector telescope described in the text.
3. Raw spectrum of protons at 45° from a 2.4 mg/cm^2 aluminum radiator bombarded with 14 MeV neutrons. The dots are data with the radiator in, the crosses with the radiator out. The acceptance of the spectrometer in arbitrary units is given by the solid line.
4. Proton production cross section and spectrum at 45° for 14 MeV neutrons incident on aluminum. The horizontal lines denote the full-width at half maximum of the acceptances of the spectrometer for the different magnet settings used.
5. Proton spectrum at 0° for 14 MeV neutrons incident on CD_2 . The peak is due to the neutron-neutron final state interaction. The horizontal lines denote the full-width at half maximum of the acceptance of the spectrometer for the different magnet settings used.
6. Best resolution spectrum of protons at 0° from neutrons incident on CH_2 . The accelerator energy was $E_{p+} = 200 \text{ KeV}$ and the neutron production angle was 98° . The dispersion is 16.3 keV/channel .

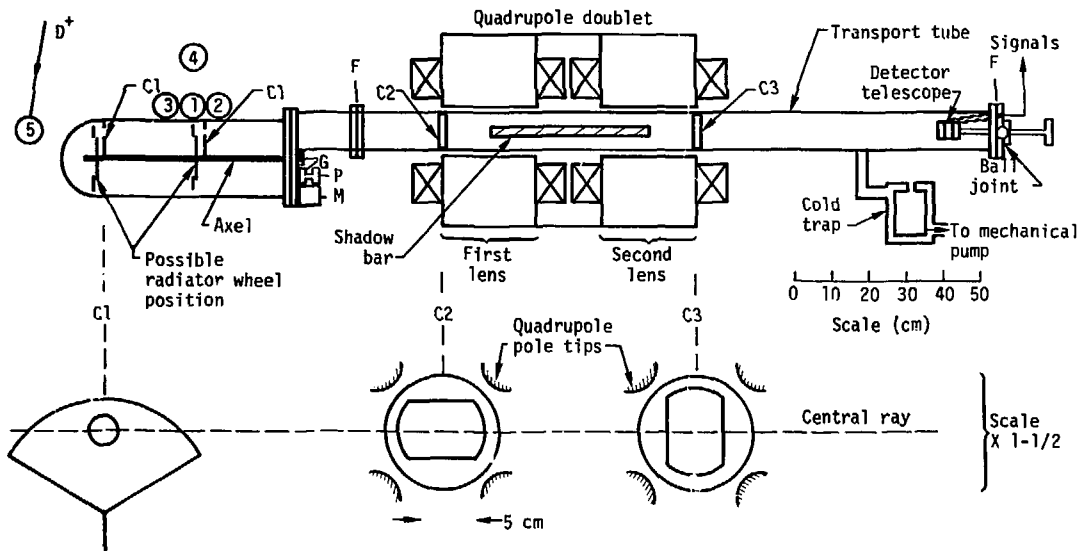


Fig. 1

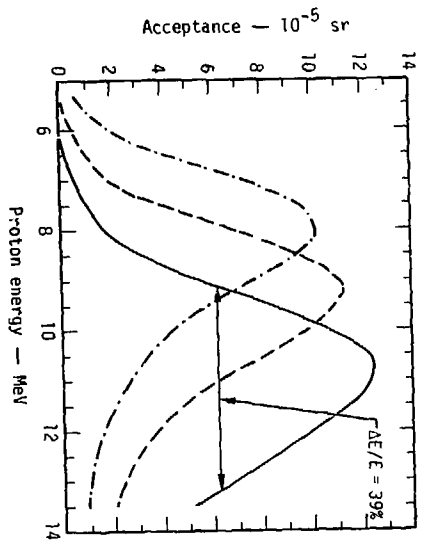


Fig. 2

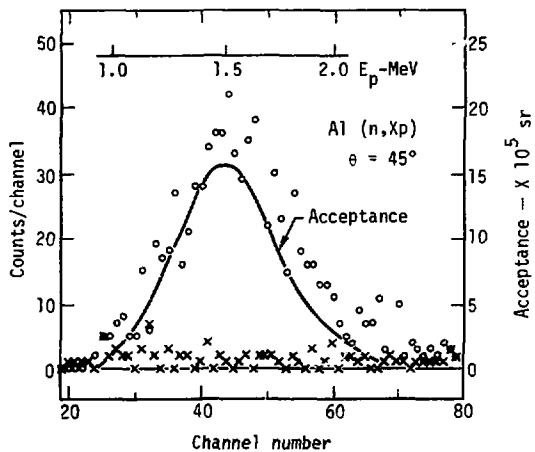


Fig. 5

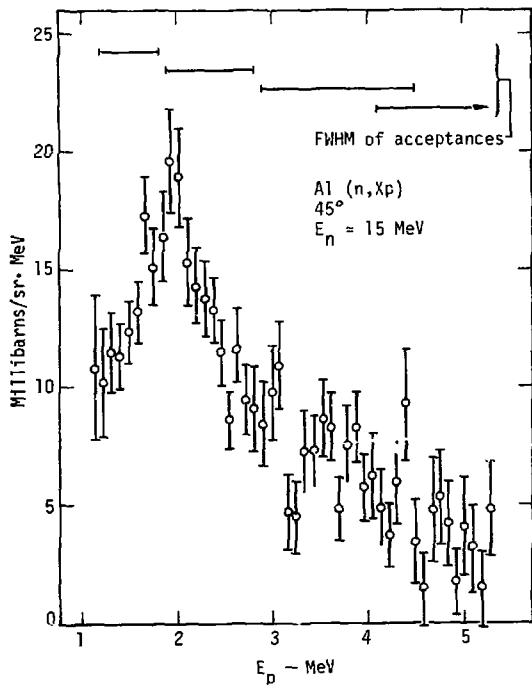


Fig. 4

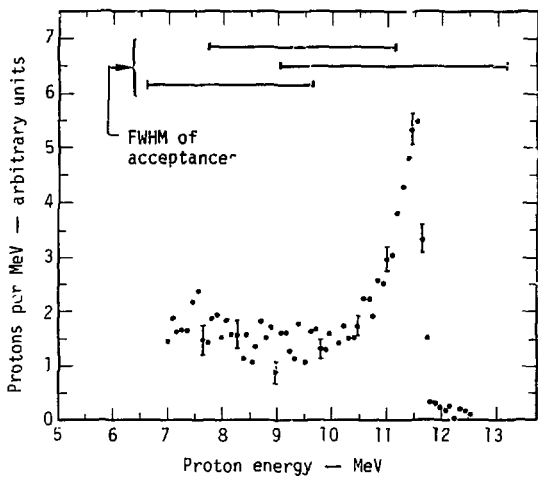


Fig. 5

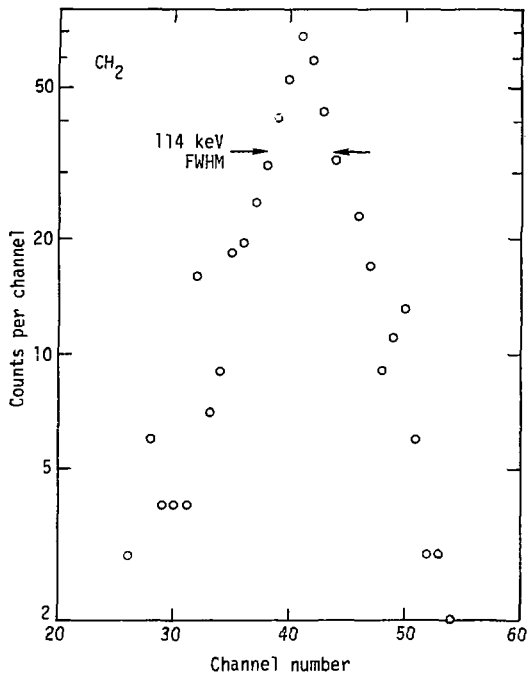


Fig. 6